ELSEVIER

Chemical Engineering Journal 68 (1997) 11–27

Chemical Engineering Journal

An integral–spectral approach for convective–diffusive mass transfer with chemical reaction in Couette flow Mathematical formulation and numerical illustrations

Zheng Chen, Pedro Arce *

Department of Chemical Engineering, FAMU-FSU College of Engineering, Florida A&M University and Florida State University, 2525 Pottsdamer Street, Tallahassee, FL 32310-6046, USA

Received 24 April 1996; revised 24 February 1997; accepted 26 March 1997

Abstract

The convective–diffusive mass transfer problem with chemical reaction in a Couette planar flow has been analyzed in terms of the integral–spectral methods originally introduced by Arce et al. (Comput. Chem. Eng. 2 (11) (1988) 1103). The problem is solved by inverting the differential model into an integral equation of a Volterra type, in the axial variable, and of the Fredholm type, in the radial coordinate. The kernel of such an integral equation is given by the Green function which does not contain any of the kinetic parameters of the (homogeneous and/or heterogeneous) reaction term. This Green function is computed in terms of the eigenfunctions and eigenvalues of the Stürm–Liouville problem associated with the radial variable. The Stürm–Liouville problem is solved (analytically) by using Airy functions and the final integral equation must be solved by an iteration procedure. Several of the mathematical formulation details are discussed and many numerical examples are presented to illustrate the technique: for example, concentration profiles for systems with heterogeneous (wall) catalytic reactions, homogenous (global) reactions and simultaneous (global and wall catalytic) reactions with kinetics of a general form, i.e. power-law and Langmuir–Hinshelwood types of functions are investigated. The solutions to the class of problems considered here are obtained as particular cases of the general integral equation solution of the differential model discussed in the article. The effects of relevant parameters in the system on the computational algorithm with respect to convergence and (numerical) stability characteristics are discussed. © 1997 Elsevier Science S.A.

Keywords: Integral–spectral methods; Convective-diffusive transport and reaction; Fourier series; Couette flows with reaction; Eigenvalues and Eigenvectors with airy functions

1. Introduction

Convective–diffusive mass transfer with homogeneous and heterogeneous chemical reaction for different reactor designs has been analyzed under rather simplified assumptions. Cleland and Wilhelm [1] investigated first-order homogeneous reactions for a laminar tubular reactor by using a differential mathematical model which was solved by finite difference method. Lawerier [2] studied the convective–diffusive transport in Poiseuille flows coupled with a first-order homogeneous reaction. This author presented the solution in terms of analytical functions for the tubular reactor geometry. Dranoff [3] obtained solutions for convective transport and diffusion of the reactant with a catalytic wall reaction in a tubular or annular reactor by a computational scheme. In his solution approach, eigenfunctions and eigenvalues of the Stürm–Liouville problem associated with the diffusion operator were used. The eigenfunctions and eigenvalues, however, were calculated numerically. Poirier and Carr [4] extended the solution of Cleland and Wilhelm to include second-order reactions. Ogren [5] proposed a solution for the laminar tubular reactor with a first-order homogeneous and wall reactions. Solbrig and Gidaspow [6] considered a first order heterogenous reaction for a reactor with planar geometry and obtained the concentration profile as well as asymptotic expressions for large eigenvalues. Also, these authors used a finite difference scheme to study the case of an arbitrary wall reaction rate for a rectangular reactor [29].

Mass transfer processes containing a fluid that flows under laminar regime in a Couette fashion has a variety of applications in processes related to chemical engineering. Some of these applications include, for example, liquid–liquid extraction [7], the treatment of continuously moving solids

* Corresponding author. Tel: +1 850 487 6166; e-mail: arce@eng.fsu.edu

PII S1385-8947(97)00049-1

in the form of wires and sheets which involves moving interfaces and complex diffusion and convection mass transfer [8], coating processes [9], and some important biochemical system such as mass transfer processes in dializers, oxygenators, and other membrane processes [10].

The present paper focus on a problem related to the family mentioned above where the convective–diffusive mass transport problem is coupled with chemical reactions either at the wall or in the bulk solution. The fluid moves under a Couette type of flow in a rectangular geometry. The solution methodology adopted for the analysis of such a problem follows the general computational approach introduced by Arce et al. [11] and that more recently was extended to a variety of transport and reaction processes [12,13]. Such scheme uses integral equations whose kernel is given by the Green function of the differential problem. This Green function is obtained by a spectral expansion using the eigenvalues and eigenvectors of the linear transport problem. Within the general framework, this methodology can be viewed as an integral–spectral approach [14,13]. The methodology decouples the linear aspects of the problems from the non-linear contribution (i.e. the transport is considered separately from the reaction). As it will be shown in the analysis, a family of problems can be efficiently solved with such a type of approach with a minimum of changes in the computational aspects. The approach converts a differential model into a non-linear integral equation that is then solved on the computer by an iterative procedure.

This paper will introduce the differential model in the next section with the physical assumptions related to it. The integral formulation, with the identification of the eigenvalue and Green function, will be presented next. The following section will address the solution of the eigenvalue problem in terms of the Green function in terms of eigenvalues and eigenfunctions. Illustrations covering a variety of cases will be discussed at the end of this contribution.

2. General model formulation

A sketch of the geometry of the device used in this paper is shown in Fig. 1. Such a system displays a geometry with two parallel plates where the lower plate is assumed fixed and impermeable to mass transfer of chemical species, while the upper plate moves at a constant speed, V. The upper plate may undergo a heterogeneous catalytic reaction simultaneously with a homogeneous reaction in the bulk. The chemical reaction rate functions of both types of reactions are assumed of a general form and they are only restricted by the usual smoothness constraints necessary in kinetics. In this sense, the reaction rate could be modelled by a power-law kinetics, a Langmuir–Hinshelwood kinetics or a zero order type of reaction rate. It is also assumed that: (1) the hydrodynamic velocity field does not feature a component of the velocity field in the z-direction since there is no flow in z-direction (i.e. the flow field is one dimensional and fully developed); (2) the system is isothermal, hence the physical properties of the system remain constant; (3) the fluid is assumed to be incompressible and Newtonian; and (4) the steady state is reached. Under these assumptions, the hydrodynamic velocity profile is given by [15]

$$v_x(y) = \frac{V}{W} y \tag{1}$$

where it also is assumed that there is no pressure gradient in the system. This assumption does not represent a serious limitation of the problem and extensions to relax these assumption are not tedious. The molar species continuity equation with the bulk reaction term and under the assumptions discussed above is given by

$$v_x(y)\frac{\partial C'}{\partial x} = D\frac{\partial^2 C'}{\partial y^2} - Q'[C'y(x,y)] \tag{2}$$

with inlet and boundary conditions specified as:

$$C'(x=0) = C_0 \tag{3}$$

$$\left.\frac{\partial C'}{\partial y}\right|_{y=0} = 0 \tag{4}$$

$$-D\left.\frac{\partial C'}{\partial y}\right|_{y=W} = R'[C'(x,W)] \tag{5}$$

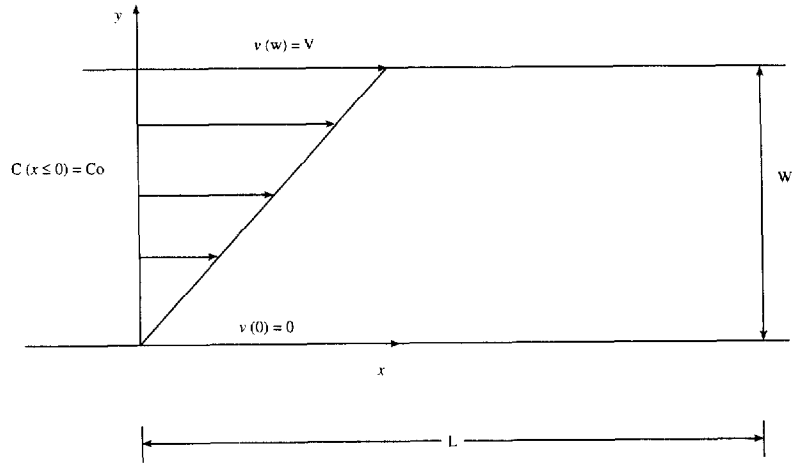

Fig. 1. Geometrical sketch of the planar Couette device.

In Eq. (2), it has been assumed that the convective transport in the axial direction is dominant with respect to diffusion in the axial direction. The function, $Q'[C'(x,y)]$ is a source(or sink) term of the species originating from the homogeneous reaction term occurring in the bulk system, and $R'[C'(x,W)]$ is another source term used to describe the heterogeneous reaction at the moving surface.

By introducing Eq. (1) in Eq. (2) and by defining the following set of non-dimensional parameters

$$\xi \equiv \frac{x}{L} \quad \rho \equiv \frac{y}{W} \quad C \equiv \frac{C'}{C_0} \tag{6}$$

$$\mathrm{Pe} \equiv \frac{VW}{D} \quad \mathrm{Ge} \equiv \frac{W}{L} \tag{7}$$

Eqs. (2)–(5) can be transformed into

$$\alpha\rho\frac{\partial C}{\partial \xi} = \frac{\partial^2 C}{\partial \rho^2} - \Omega[C(\xi,\rho)] \tag{8}$$

$$C|_{\xi=0} = 1 \tag{9}$$

$$\left.\frac{\partial C}{\partial \rho}\right|_{\rho=0} = 0 \tag{10}$$

$$\left.\frac{\partial C}{\partial \rho}\right|_{\rho=1} = -\Omega_w[C(\xi,1)] \tag{11}$$

where the parameter $\alpha \equiv \mathrm{PeGe}$ and the non-dimensional reaction terms have been identified as $\Omega[C(\xi,\rho)]$ and $\Omega_w[C(\xi,1)]$ for the bulk and wall reaction, respectively. These non-dimensional rates of reaction are given by

$$\Omega[C(\xi,\rho)] \equiv \frac{W^2}{D} Q[C(\xi,\rho)] \tag{12}$$

and

$$\Omega_w[C(\xi,1)] \equiv \frac{W}{D} R[C(\xi,1)] \tag{13}$$

Eqs. (12) and (13) will feature the Damkholer number for the case of homogeneous and heterogeneous reactions, respectively when a particular reaction rate is selected. There is no special restriction for this selection and kinetics of the power-law and Langmuir–Hinshelwood family will be used in this investigation. In the section below the differential model derived above will be inverted into the integral form and the Green function of the problem as well as the associated eigenvalue problem will be identified.

3. Solution methodology

The solution of the differential model represented by Eqs. (8)–(11) is based on the use of an integral–spectral approach that uses the Green function of the convective–diffusive transport problem of the model (see Refs. [11,13,12]) as the kernel of the integral equation for the concentration field. The reaction terms of both the catalytic reaction and the homogeneous reaction in the bulk appear in the integrals as non-linear source terms.

In this section, the analysis is focused on inverting the differential problem into an integral problem. The approach begins with (8) which can be written in a compact form by defining the following parabolic differential operation

$$H \equiv -\frac{\partial^2}{\partial \rho^2} + \alpha\rho\frac{\partial}{\partial \xi} \tag{14}$$

By using the operation defined in Eq. (14) in Eq. (8) we obtain

$$HC = -\Omega[C(\xi,\rho)] \tag{15}$$

Now, an integration by using a test function $G(\boldsymbol{x}|\boldsymbol{x}')$ is proposed to obtain

$$\int_0^{\xi+\epsilon} \mathrm{d}\xi' \int_0^1 \mathrm{d}\rho'\, G(\boldsymbol{x}|\boldsymbol{x}')HC(x') = -\int_0^{\xi+\epsilon} \mathrm{d}\xi' \int_0^1 \mathrm{d}\rho'\, G(\boldsymbol{x}|\boldsymbol{x}')\Omega[C(x')] \tag{16}$$

where $\boldsymbol{x} \equiv (\xi,\rho)$. Working on the left hand side of Eq. (16) and successively using integration by parts, yields an equation that can be written as follows

$$\begin{aligned}
&\int_0^{\xi+\epsilon} \mathrm{d}\xi' [G(\boldsymbol{x}|\boldsymbol{x}i', 1)\Omega_w[C(\xi', 1]] + G_\rho'(\boldsymbol{x}|\xi', 1) \\
&\quad \times C(\xi', 1) - G_\rho'(\boldsymbol{x}|\xi', 0)C(\xi', 0)] \\
&\quad + \int_0^{\xi+\epsilon} \int_0^1 \mathrm{d}\rho' \hat{H} G(\boldsymbol{x}|\boldsymbol{x}')C(x')\mathrm{d}\xi' \\
&\quad + \int_0^2 \alpha\rho' [G(\boldsymbol{x}|\xi+\epsilon,\rho')C(\xi+\epsilon,\rho') \\
&\quad - G(\boldsymbol{x}|0,\rho')C(0,\rho')] \\
&= -\int_0^{\xi+\epsilon} \mathrm{d}\rho' \int_1^1 \mathrm{d}\rho'\, G(\boldsymbol{x}|\boldsymbol{x}')\Omega[C(x')]
\end{aligned} \tag{17}$$

where the operation $\hat{H}$ was identified as

$$\hat{H} \equiv -\frac{\partial^2}{\partial \rho^2} - \alpha\rho\frac{\partial}{\partial \xi} \tag{18}$$

The operation $\hat{H}$ is the adjoint operation of H [16] which has been defined by Eq. (14). Eq. (17) is a general expression that holds for any boundary conditions. Mathematically, it is convenient to identify the following conditions for the test function $G(\boldsymbol{x}|\boldsymbol{x}')$ [17]

$$\hat{H}G(\boldsymbol{x}|\boldsymbol{x}') = \alpha\delta(\rho-\rho')\delta(\xi-\xi') \tag{19}$$

$$G'(\boldsymbol{x}|\xi',1) = 0 \tag{20}$$

$$G'(\boldsymbol{x}|\xi',0) = 0 \tag{21}$$

$$G(\boldsymbol{x}|\rho',\xi+\epsilon) = 0 \quad \text{(causality)} \tag{22}$$

in which $\delta(\rho-\rho')$ and $\delta(\xi-\xi')$ are the generalized Dirac delta functions. The formal integral representation results from substituting Eqs. (18)–(21) into Eq. (17) and then performing the limits operation $\epsilon \to 0$, which produces the following result

$$C(\xi,\rho) = -\frac{1}{\alpha}\int_0^{\xi} d\xi' \int_0^1 d\rho'\, G(\boldsymbol{x}|\boldsymbol{x}')\Omega[C(x')] - \frac{1}{\alpha}\int_0^{\xi} d\xi'\, G(\boldsymbol{x}|\xi',1)\Omega_w[C(\xi',1)] + \int_0^1 \rho' \times G(\boldsymbol{x}|0,\rho')C(0,\rho')\, d\rho' \tag{23}$$

In Eq. (23), the first term on the right hand side is the term that comes from the bulk reaction, the second one is due to the catalytic reaction on the wall, and the third term is the contribution from the inlet concentration distribution. Eq. (23) is a formal solution to the differential problem since the unknown, $C(\xi,\rho)$, is under the integral symbol as well as on the left hand side. Therefore, Eq. (23) requires further effort to obtain the concentration field. Also, the test function $G(\boldsymbol{x}|\boldsymbol{x}')$ is the Green function associated with the parabolic transport operator, $\hat{H}$, and it will be identified in terms of the eigenvalues and eigenfunctions of the problem. This analysis is presented in the sections below.

3.1. Identification of the associated eigenvalue problem

The integral representation of the differential problem given by Eq. (23) requires the function $G(\boldsymbol{x}|\boldsymbol{x}')$ to be identified and computed in terms of known quantities. An important step to achieve this purpose is the identification of the eigenvalue problem associated with the "lateral" diffusion processes of the physical problem.

In order to identify the proper Stürm–Liouville problem, i.e. the set of equations that leads to the eigenvalue problem, another test function $\phi_n(\rho)$ and a solution $U(\xi)$ will be used. The set of function $\phi_n(\rho)$ satisfies *only the homogeneous boundary conditions* of the problem given in Eqs. (8)–(11).

By using the operator H with the homogeneous boundary conditions by successive integrations by parts of Eq. (15), the following Stürm–Liouville problem can be obtained

$$\frac{d^2\phi_n}{d\rho^2}(\rho) = -\lambda_n^2\rho\phi_n(\rho) \tag{24}$$

$$\phi_n'(1) = 0 \tag{25}$$

$$\phi_n'(0) = 0 \tag{26}$$

Eqs. (24) and (25) are the homogeneous boundary conditions for the problem in terms of function $\{\phi_n(\rho)\}$ and have been derived from the non-homogeneous boundary conditions of the original problem. The problem given by Eqs. (24)–(26) defines the Stürm–Liouville problem associated with the diffusion process in the transverse direction, ρ, of the channel.

Now, with the definition of the set of function $U_n(\xi)$ given by

$$U_n(\xi) \equiv \int_0^1 d\rho'\, \rho'\phi_n(\rho')C(x') \tag{27}$$

and the set functions $I_n(\xi)$ given by

$$I_n(\xi) \equiv -\int_0^1 d\rho'\, \phi_n(\rho')\Omega[C(x')] \tag{28}$$

the following ordinary differential equation can be written

$$\lambda_n^2 U_n(\xi) + \alpha\frac{dU_n}{d\xi}(\xi) = 0 \tag{29}$$

This equation is subject to an initial condition, $U_n(0)$ that is constructed by using the original initial condition given by Eq. (27) to obtain

$$U_n(0) = \int_0^1 d\rho'\, \rho'\phi_n(\rho')C(0,\rho') \tag{30}$$

The solution to Eq. (29) is given by

$$U_n(\xi) = U_n(0)\exp\left[-\left(\frac{\lambda_n^2\rho}{\alpha}\right)\right] + \int_0^{\xi}\frac{I_n(\xi')}{\alpha}\exp\left[\frac{\lambda_n^2}{\alpha}(\xi'-\xi)\right]d\xi' \tag{31}$$

in which the set of eigenfunctions $\phi_n(\rho)$ with eigenvalues λ_n is the solution to the eigenvalue problem defined by Eqs. (24)–(26). This set of functions is a basis where the elements that belong to two different eigenvalues are orthogonal to each other with a weighting function ρ on the interval (0, 1). Therefore,

$$\int_0^1 d\rho'\, \rho'\phi_n(\rho')\phi_m(\rho') = A_n^2\delta_{nm} \tag{32}$$

where

$$A_n^2 = \int_0^1 d\rho'\, \rho'\phi_n^2(\rho') \tag{33}$$

is the normalization factor of the set of eigenfunctions $\{\phi_n(\rho)\}$. The set of functions $\{\phi_n(\rho)\}$ and λ_n are the eigenfunctions and eigenvalues respectively of the characteristic

equation. This characteristic equation may be derived by proposing a general solution to Eq. (24) in terms of the Airy functions $A_i(z)$ and $B_i(z)$ of first and second kind, respectively. In order to achieve this solution, the following transformation of variables is proposed [18]

$$z=\lambda_n^{2/3}\rho \text{ and } U_n(z)\equiv\phi_n(\lambda_n^{2/3}z) \tag{34}$$

which can be used in Eq. (24) to yield

$$U_n''(z)-zU_n(z)=0 \tag{35}$$

Eq. (35) is a standard Airy differential equation (see, for example, Ref. [19]. The general solution to eq. (35) can be written as

$$U_n(z)=C_1A_i(z)+C_2B_i(z) \tag{36}$$

where C_1 and C_2 are integration constants. The values of C_1 and C_2 must be determined from the boundary conditions of the eigenvalue problem. Invoking Eqs. (25) and (26), the following characteristic equation may be obtained

$$\sqrt{3}A_i'(-\lambda_n^{2/3})+B_i'(-\lambda_n^{2/3})=0 \tag{37}$$

where the prime is used to denote differentiation with respect to z. The eigenfunctions for the eigenvalue problem associated with diffusive transport problem in the transverse direction of the channel are

$$\{\phi_n(z)\}=\left\{\left[A_i(z)+\frac{1}{\sqrt{3}}B_i(z)\right]_{z=-\lambda^{2/3}\rho}\right\} \tag{38}$$

By using the integral representation of the derivatives of the Airy functions $A_i'(z)$, $B_i'(z)$ [30] and the computational approach introduced by Chen et al. [18] numerical values for the eigenvalues and eigenfunctions have been obtained from Eqs. (37) and (38) respectively. Table 1 gives the first fifty eigenvalues. The eigenvalues increase monotonically with a slow rate of increase for the small values of n but this rate increases for larger values of n. For example, the difference between λ_2 and λ_3 is 70.3114, but between λ_{41} and λ_{42}, the difference is 1805.1. Hence, the larger λ_n, the more rapidly the series expansion for concentration profiles will converge with a small number of terms.

Figs. 2 and 3 show the graphical presentation of the first ten eigenfunctions. Generally, oscillations of the eigenfunction about zero increase as the order of the eigenfunction increases. The homogeneous boundary conditions of zero flux are satisfied at both ends of the domain by the variable $\rho(0<\rho<1)$. The increase in frequency of the eigenfunctions suggests an interesting criteria for the number of points required in the variable ρ to capture (numerically) the behaviour of the eigenfunctions. The eigenfunctions $\phi_n(\rho)$ are all analytical and they are based on the Airy functions as discussed previously. The fact that the eigenfunctions of the associated Stürm–Liouville problem are given in terms of analytical functions is very useful from the computational point of view. Also, the eigenvalues are independent of the main physical parameters of the system (i.e. D_{aw}, D_a and α).

Table 1
First fifth eigenvalues of the operator L

N	λ	N	λ
1	0.000000E+00	26	0.139714E+05
2	0.256381E+02	27	0.151076E+05
3	0.959495E+02	28	0.162882E+05
4	0.210681E+03	29	0.175132E+05
5	0.369821E+03	30	0.187828E+05
6	0.573388E+03	31	0.200967E+05
7	0.821352E+03	32	0.214550E+05
8	0.111375E+04	33	0.228577E+05
9	0.111375E+04	34	0.243048E+05
10	0.183176E+04	35	0.257964E+05
11	0.225736E+04	36	0.273322E+05
12	0.225739E+04	37	0.289128E+05
13	0.324188E+04	38	0.305375E+05
14	0.380075E+04	39	0.322068E+05
15	0.380075E+04	40	0.339201E+05
16	0.505172E+04	41	0.356757E+05
17	0.574359E+04	42	0.374808E+05
18	0.648035E+04	43	0.393276E+05
19	0.726128E+04	44	0.412189E+05
20	0.808662E+04	45	0.431547E+05
21	0.895638E+04	46	0.451346E+05
22	0.987051E+04	47	0.471592E+05
23	0.108291E+05	48	0.495581E+05
24	0.118322E+05	49	0.513414E+05
25	0.128797E+05	50	0.534991E+05

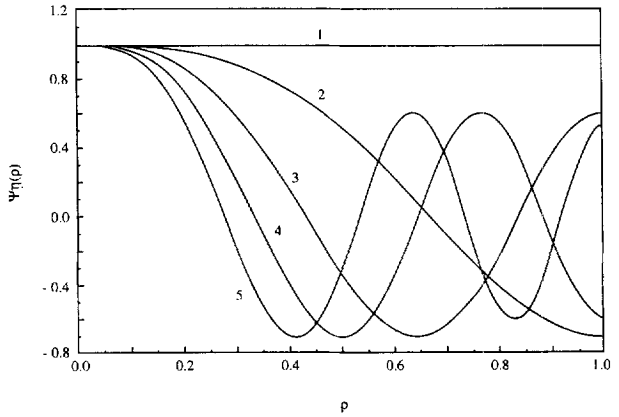

Fig. 2. First five eigenfunctions of the Stürm–Liouville problem.

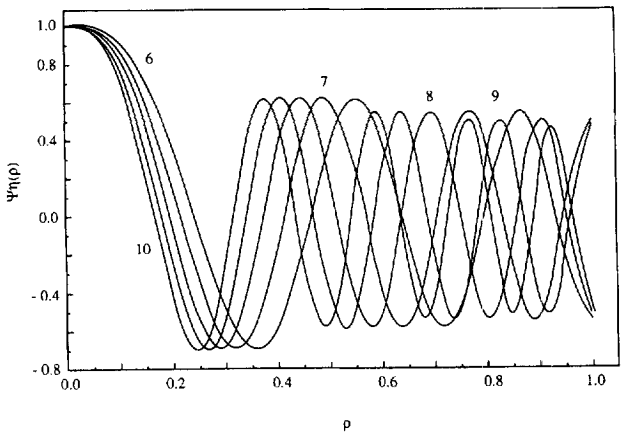

Fig. 3. Next ($n=5$–10) eigenfunctions of the Stürm–Liouville problem.

This aspect is useful in the parametric analysis of the original system as it eliminates the need to recompute the eigenvalues and eigenfunctions every time that the kinetic parameters are changed as it will be presented in the applications of this contribution.

3.2. Expansion of the Green function in the set of eigenfunctions

The Green function $G(\boldsymbol{x}|\boldsymbol{x}')$ is formally identified in this section. In the section below, the analysis will be focused on producing a computational formula for the Green function. The basis for such an expansion is given by the Mercier theorem (see, for example, [20]) which allows us to compute the function $G(\boldsymbol{x}|\boldsymbol{x}')$ in terms of the eigenvalues and eigenfunctions of the Stürm–Liouville problem solved in Section 3.1.

By using the linear superposition method [17], an expansion of $C(x)$ in a series of the eigenfunctions $\phi_n(\rho)$ is given by

$$C(x) = \sum_{n=0}^{\infty} \frac{1}{A_n^2} U_n(\xi)\phi_n(\rho) \tag{39}$$

and by substituting the expression of $U_n(\xi)$ into Eq. (39), the following result is obtained

$$C(x) = \sum_{n=0}^{\infty} A_n^{-2}\left[\int_0^1 \mathrm{d}\rho'\, \rho'\phi_n(\rho')\exp\left(\frac{\lambda_n^2}{\alpha}\xi\right)\xi_n(\rho) + \frac{1}{\alpha}\int_0^{\xi} \mathrm{d}\xi'\, I_n(\xi')\exp\left(\frac{\lambda_n^2}{\alpha}(\xi'-\xi)\right)\phi_n(\rho)\right] \tag{40}$$

This equation can also be written as

$$C(x) = \int_0^1 \rho'\mathrm{d}\rho'\left[\sum_0^{\infty} A_n^{-2}\exp\left(-\frac{\lambda_n^2}{\alpha}\xi\right)\phi_n(\rho')\psi_n(\rho')\right] - \frac{1}{\alpha}\int_0^{\xi}\mathrm{d}\xi'\int_0^1 \mathrm{d}\rho'\,\Omega[C(x')]\left[\sum_0^{\infty} A_n^{-2}\exp\left(\frac{\lambda^2}{\alpha}(\xi'-\xi)\right)\times\phi_n(\rho')\phi_n(\rho')\right] \tag{41}$$

By comparing term by term between Eqs. (41) and (23) the following expression for $G(\boldsymbol{x}|\boldsymbol{x}')$ can be derived

$$G(\boldsymbol{x}|\boldsymbol{x}') = \sum_0^{\infty} A_n^{-2}\left[\exp\left(\frac{\lambda_n^2}{\alpha}(\xi'-\xi)\right)\times\phi_n(\rho)\phi_n(\rho')\theta(\xi-\xi')\right] \tag{42}$$

where $\theta(\xi-\xi')$ is a step function and A_n^2 is the normalization factor defined by Eq. (42).

The function $G(\boldsymbol{x}|\boldsymbol{x}')$ given by Eq. (32) satisfies all the properties required by Eqs. (19)–(22). Therefore, by definition [16], the function $G(\boldsymbol{x}|\boldsymbol{x}')$ is the Green function of the differential problem of diffusive–convective transport and reaction formulated in Section 2. With the identification of the Greens's function the integral formulation of the problem is now complete.

4. Computational approaches to solve the integral equation of the concentration field

The concentration field equation given by Eq. (41) is a formal nonlinear equation that requires a computational solution to obtain the values of $C(\rho, \xi)$. The general form of this integral equation is given by

$$W(x) = W(x^{\circ}) + \int_{(x)} \mathrm{d}x'\, K(\boldsymbol{x}|\boldsymbol{x}')F[W(x)] \tag{43}$$

where $K(\boldsymbol{x}|\boldsymbol{x}')$ is the kernel of the integral transformation which is given by the Green function identified in Section 3. The notation $W(\boldsymbol{x})$ has been used to indicate a generic concentration profile for the various cases (i.e. wall reaction, bulk reaction, etc.) involved in the physical system. The function $F[W(\boldsymbol{x})]$ represents a generic kinetic law. In the most general case, Eq. (43) is a Hammerstein–Volterra nonlinear integral equation [21] of the second kind. The nonlinear aspects featured by Eq. (43) are introduced by the potential nonlinear kinetics such as power law (with $n \geq 2$), Langmuir–Hinshelwood, or others. The solution to Eq. (43) can be obtained by a variety of methods including a modified block by block method [22], spline approximations [23] and others (see for example, Golberg [21] for a recent review). The equation can also be solved by an iterative procedure of the form

$$W^{(k+1)}(\boldsymbol{x}) = W(x^{\circ}) + \int_{(x)} \mathrm{d}x'\, K(\boldsymbol{x}|\boldsymbol{x}')F[W^k(\boldsymbol{x}')] \tag{44}$$

One successful technique is the Piccard iteration procedure that has been used in convective–diffusive transport problems [13,12]. For cases where the kinetics is not a function of the concentration field, i.e. zero order kinetics, the solution to the integral equation can be accomplished without an iteration procedure of any kind. For the cases with reactions at the wall, the computational solution must be carefully handled to eliminate the so-called Gibbs phenomena. This produces spatial oscillations in the concentration field because of the need for a large number of eigenvalues required to reproduce the profile near the wall [12]. The procedure used in this contribution is based on the replacement of Fourier expansions by closed sums identified by solving an asymptotic convective–diffusive problem with zero order reaction at the wall [24]. The approach follows the general guidelines explained in Ref. [12] and successfully applied to the Poiseuille flow case [13].

Several details about the illustration, of the various cases are included in the sections below. Some mathematical aspects that are not essential to the discussion in the text are

included in Appendix A. These aspects, however, are useful for the implementation of the solution from the numerical point of view.

As discussed above, the concentration profile may be obtained by solving the (formal) integral representation of the differential problem. In general, such a solution will require the use of a 2-D grid in the axial and transversal directions in the channel. However, the solution for the case of the wall reactions can be obtained by a computational approach that involves the calculation of the concentration at the wall only, i.e. $C(1,\xi)$. This characteristic is based on the fact that catalytic wall reactions produce integrals with the unknown only at the surface of the channel. This is very useful as it reduces the iterative procedure to only one dimension, i.e. the axial variable, rather than the two dimensions originally featured by the problem. Several iterative procedures can be used to obtain the solution of integral equations of the type of Eq. (43). In this paper, a procedure based on the following equation

$$C^{n+1}(\xi,\rho)=\frac{C^{n}(\xi,\rho)}{C^{n}(\xi,\rho)+|\tilde{O}[C^{(n)}(\xi,\rho)]|} \tag{45}$$

was adopted. The function $\tilde{O}(\cdot)$ in Eq. (1) is given by

$$\tilde{O}[C^{(n)}(\xi,\rho)]=\frac{1}{\alpha}\int_0^1 G(\xi,\rho|\xi',1)\Omega_w(\xi',1)\,d\xi'$$

$$+\frac{1}{\alpha}\int_0^{\xi}\int_0^1 G(\xi,\rho|\xi',\rho')\Omega(\xi',\rho)\,d\xi'\,d\rho' \tag{46}$$

and $C^{(n)}$, $C^{(n+1)}$ are respectively the concentration profiles calculated in the nth and $(n+1)$th iterations. Eq. (45) was solved numerically for the various cases in terms of above iterative scheme. A mesh with at size of 51×51 in 2D ξ, ρ-plane was chosen to perform the computations when necessary. This mesh size was shown to be small enough to reach solutions within a prescribed error. Convergent solutions were taken if the following condition was satisfied

$$\left(\sum_{j=1}^{N}\sum_{i=1}^{M}\frac{[C^{(n+1)}(\xi_i,\rho_j)-C^{n}(\xi_i,\rho_j)]^2}{(NM-1)}\right)^{1/2}<\epsilon \tag{47}$$

where, $N=51$, $M=51$ and ϵ is the permitted convergent error ($\epsilon=10^{-5}$).

The Green function $G(\xi,\rho|\xi',\rho')$ in Eq. (46) contains an infinite number of terms which is not possible to be included in the computations. However, since each term of the function is expanded in terms of an infinite series of eigenfunctions and since each term is associated with exponential function of ξ that decays with ξ and the eigenvalue λ_n, an adequate cut can be obtained for taking into account only a finite number of the terms. Therefore, the Green function $G(\boldsymbol{x}|\boldsymbol{x}')$, tends rapidly to zero with increasing corresponding eigenvalues when $\xi>0$ within the domain of calculation and for a given value of ξ. For the conditions involved in this study, a number of twenty terms were found to give results within the required accuracy. All numerical integrals involved were evaluated by the Simpson's method of integration except for the first two steps where a trapezoidal method was found to give a better result.

There are three types of errors involved in the complete solution of the integral of Eq. (45). The first error is associated with the implementation of the Green function in the computer calculations. We will denote this error by ϵ_1. As pointed out previously a value of $N=20$ in terms of the series expansion for the Green functions indicates that the series captures the behaviour of the function. Another error is the one involved in the numerical calculations of the integrals of the equation. This error is related to the particular method used in the numerical calculation of such integrals. We denote this error with ϵ_2 is a function of the size of the integration mesh. For most of the calculations (after some trial and error) a number of 50 points were enough for both the radial and axial variables. However, for the case of wall reactions of the axial variable is the only one to be considered with as pointed out earlier in this section. The final error that needs attention is the error associated with the iterative procedure described above in this section. If we denote this error by ϵ_3, we have a error relationship such that the total error is given by

$$\epsilon_t=\epsilon_1+\epsilon_2+\epsilon_3 \tag{48}$$

A good criteria for achieving meaningful calculations is that $\epsilon_1<\epsilon_2<\epsilon_3$.

Based on the successive iteration approach mentioned above, the proposed method is absolutely convergent for any initial concentration profile. In most of the cases, an error ϵ_3 of 10^{-5} could be reached after 10–20 iterations. The computations were improved by recognizing that the Green function $G(\xi,\rho|\xi',\rho')$ is independent of the parameters of the model (Pe, Da and Ge) hence the value of $G(\xi,\rho|\xi',\rho')$ can be retained in computations for different values of the parameters. Substituting the expression for the Green function into Eq. (23) and rearranging the equation, we have

$$C(x)=1-\frac{1}{\alpha}\sum_n^{\infty}A_n^{-2}\phi_n(\rho)\exp\left(-\frac{\lambda_n^2}{\alpha}\xi\right)\int_0^{\xi}\exp\left(\frac{\lambda_n^2}{\alpha}\xi'\right)d\xi'$$

$$\times\left[\int_0^1 d\rho'\,\phi_n(\rho')\Omega[C(\xi',\rho')\right]$$

$$+\phi_n(1)\Omega_w[C(\xi',1)] \tag{49}$$

The values the function $G(\boldsymbol{x}|\boldsymbol{x}')$ for each point in the constituted mesh where calculated once, and then stored as a data file, which could be retrieved in the later computation for other sets of the parameters. By using this strategy, computations for heterogeneous and homogeneous problems with an error of 10^{-5} could be performed in a relatively short time for a wide range of values of the parameters involved in the model.

In the previous paragraphs, the general iterative scheme to obtain the convergent solution of the integral Eq. (49) was

described. Such a procedure, however, shows fluctuations in the concentration profile near the vicinity of the catalytic surface of the moving plate when a heterogeneous reaction takes place. This is known as the Gibbs phenomenon [16], is caused by the discontinuity of the function of $C(\xi,\rho)$ at the position of $\rho=1$, where the eigenfunction series expansion requires a great number of terms because of its very slow convergence. Several methods have been proposed to overcome the effect, among those, a close form expression of the series expansion [12] has been used to correct the behaviour of the series near the reactor wall. In this approach, an asymptotic result for the sum of the remainder of the series is derived so that the calculation can be conducted by taking the summation of a limited number of terms of the "closed" form. In Appendix A, the derivation of the "closed" form expression for the case of the heterogeneous reaction term is presented.

The formal solution of the general convective–diffusive transport problem is given by

$$C(\xi,\rho)=\int_0^1 \rho' G(\boldsymbol{x}|0,\rho')C(0,\rho')\,d\rho' - \frac{1}{\alpha}\int_0^{\xi} d\xi' \int_0^1 d\rho' \times G(\boldsymbol{x}|\boldsymbol{x}')\Omega[C(x')] - \frac{1}{\alpha}\int_0^{\xi} d\xi' G(\boldsymbol{x}|\xi',1) \times \Omega_w[C(\xi',1)] \quad (50)$$

However, since there is no homogeneous reaction in the bulk fluid Eq. (50) can be rewritten as

$$C(\xi,\rho)=\int_0^1 \rho' G(\boldsymbol{x}|0,\rho')C(0,\rho')\,d\rho' - \frac{1}{\alpha}\int_0^{\xi} d\xi'\, G(\boldsymbol{x}|\xi',1)\Omega_w[C(\xi',1)] \quad (51)$$

$G(\boldsymbol{x}|\boldsymbol{x}')$ is the Green function associated with the transport problem and it is given by

$$G(\boldsymbol{x}|\xi',1)=\sum_{n=0}^{\infty} A_n^{-2}\left[\exp\left(\frac{\lambda_n^2}{\alpha}(\xi'-\xi)\right) \times \phi_n(\rho)\phi_n(1)\right]\theta(\xi-\xi') \quad (52)$$

Eq. (51) is the solution for the heterogeneous catalytic reaction case described above. The integral equation contains two terms. The first one is the contribution from the inlet concentration distribution and the second one is the term related to the contribution of the reaction at the wall. If a reactant is fed to the system with a uniform concentration (i.e. $C_0=1$ at $\xi=0$), then substituting the expression for $G(\boldsymbol{x}|0,\rho')$ into the first term of Eq. (51) leads to

$$\int_0^1 \rho' G(\boldsymbol{x}|0,\rho')\,d\rho' = \sum_{n=0}^{\infty} A_n^{-2}\phi_n(\rho)\exp\left(-\frac{\lambda_n^2}{\alpha}\xi\right)\gamma_n \quad (53)$$

where

$$\gamma_n \equiv \int_0^1 d\rho'\ \rho'\phi_n(\rho') \quad (54)$$

γ_n can be related to the boundary condition at the wall, $\rho=1$, by using the eigenvalue problem identified in Section 3.2 by following the methodology described in Ref. [13].

$$\gamma_n = 0 \quad \text{for all } n\neq 0 \quad (55)$$

$$\gamma_n = \frac{\sqrt{2}}{2} \quad \text{for } n=0 \quad (56)$$

Eqs. (55) and (56) can be proved by using $\phi_n'(1)=0$, $n\geq 1$. For the case of $n=0$, $\lambda_0=\sqrt{2}$ for the normalized zero eigenfunction. The result of this analysis is that

$$\int_0^1 \rho' G(\boldsymbol{x}|0,\rho')\,d\rho' = 1 \quad (57)$$

For the case of uniform concentration distribution at the inlet. Therefore, the general solution for heterogeneous catalytic reaction with an uniform inlet distribution is a non-linear equation with the wall concentration as the unknown. This leads to the solution of a boundary-integral equation which reduces by one the spatial dimension of the original differential problem. This equation is given by

$$C(x)=1-\frac{1}{\alpha}\int_0^{\xi} d\xi'\, G(\boldsymbol{x}|\xi',1)\Omega_w[C(\xi',1)] \quad (58)$$

Although the method is by no means restricted to irreversible chemical reactions, in this paper the computational approach will focus on irreversible reactions of power-law and Langmuir–Hinshelwood kinetics.

For the case of power-law reaction kinetics with an arbitrary choice of order, n, the reaction rate is given by

$$R[C'(\xi,1)]=k_w C'^n(\xi,1) \quad (59)$$

where k_w is the reaction constant of the heterogeneous catalytic reaction. The non-dimensional form to the reaction rate kinetics is

$$\Omega_w[C(\xi,1)]=D_{aw}C^n(\xi,1) \quad (60)$$

where $D_{aw}\equiv k_w W/D$ is the Damkholer number, which describes the relative importance of the chemical reaction to diffusion.

Hence, for the case of the chemical reaction mentioned in Eq. (60), Eq. (58) becomes

$$C(x)=1-\frac{D_{aw}}{\alpha}\int_0^{\xi} d\xi'\, G(\boldsymbol{x}|\xi',1)C^n(\xi',1) \quad (61)$$

Another example of heterogeneous catalytic reactors considered here is the Langmuir–Hinshelwood form. The expression corresponding to this kinetics is given by

$$R[C'(x,1)] = \frac{k_w C_w'(x)}{\hat{K} + C_w'(x)} \tag{62}$$

where k_1 is the kinetic constant, $\hat{K}$ is the equilibrium (absorption–desorption) constant, and $C_w'(x)$ is the concentration of the reactant at the moving wall of the system. The non-dimensional version of this equation is

$$\Omega_w[C(\xi,1)] = \frac{D_{aw} C(\xi,1)}{K + C(\xi,1)} \tag{63}$$

Similarly as in Eq. (60), D_{aw} is the Damkholer number and K is a non-dimensional constant.

Substituting Eq. (63) into Eq. (58) yields

$$C(x) = 1 - \frac{D_{aw}}{\alpha} \int_0^{\xi} d\xi'\, G(x|\xi',1) \frac{C(\xi',1)}{[K + C(\xi',1)]} \tag{64}$$

Eq. (64) has two important limiting forms. The case of zero order reaction limit is achieved when $C(\xi',1) \gg K$ and then Eq. (64) reduces to

$$C(x) = 1 - \frac{D_{aw}}{\alpha} \sum_{n=0}^{\infty} \frac{\phi_n(\rho)\phi_n(1)}{A_n^2} \int_0^{\xi} d\xi' \times \exp[-\beta_n(\xi - \xi')] \tag{65}$$

where $\beta_n \equiv \lambda_n^2/\alpha$. Eq. (65) has the same form as the zero order reaction with the power law kinetics (i.e. Eq. (60) with $n=0$).

After integration, and use of the zero eigenvalues (i.e. $\lambda_0 = 0$) and corresponding eigenfunctions (i.e. $\phi_0(\rho) = \sqrt{2}$), Eq. (65) produces the following explicit solution for the concentration profile system for the zero order reaction case.

$$C(x) = 1 - \left(\frac{2D_{aw}}{\alpha}\right)\xi - \left(\frac{D_{aw}}{\alpha}\right) \sum_{n=1}^{\infty} \frac{\phi_n(1)}{\beta_n} \phi_n(\rho) \times [1 - \exp(-\beta_{n\xi})] \tag{66}$$

Another limiting case is the first order reaction limit (when $C(\xi',1) \ll K$). This implies that the solution to the system is given by

$$C(x) = 1 - \frac{D_{aw}}{\alpha K} \int_0^{\xi} dG(x|\xi',1)\, C(\xi',1) \tag{67}$$

which has the same form as Eq. (61) when take $n = 1$.

Eqs. (61) and (64) are integral representations of the problem for the convective–diffusive transport and power-law or Langmuir–Hinshewood kinetics for the surface reaction, respectively. Eqs. (66) and (67) are the solution of two interesting limiting cases of the physical problem.

In order to obtain the concentration profile, the integral equation written above will be solved by a computational scheme explained above. The Gibbs phenomena at the wall of the reactor will be properly handled to produce the correct numerical results by using the approach outlined earlier in this Section 2 and in Appendix A.

Numerical solutions of Eqs. (61) and (64) have been obtained and concentration profiles obtained, for different values of the parameters (i.e. D_{aw}, n, K) and for different reaction kinetics (i.e. power-law and Langmuir–Hinshelwood types).

The relative effect of the convective transport with respect to the diffusive transport in the system is characterized by the parameter Pe, which is defined in Eq. (7) of this article. It has been shown that [25,26], axial diffusion becomes insignificant when Pe > 100. For Pe < 100, a decrease in the value of the Peclet number will increase the effect of axial diffusion. There is however, a wide class of practical problems where the axial dispersion play a negligible role. Hence, in this work, we keep the Pe ≥ 100, and neglect the axial diffusion compared with the convective transport in the axial direction. The other parameters investigated in this work are α in the range 1–100 D_{aw}, and the reaction order $N = 1,2,3$.

Fig. 4(a) and (b) shows the effect of the order of the wall reaction, n, on the concentration profiles when a kinetics of the power-law type is used in the reaction rate and the values of the parameters are given by $\alpha = 10$ and $D_{aw} = 1$. As the value of n decreases from 3 to 0, the concentration of reactant decreases indicating an increase in the effect of the wall reaction. For decreasing value of n, the reaction rate increases. Fig. 4(a) shows that the concentration profiles at the exit position of the reactor ($\xi = 1$) along the lateral direction are very close to each other. The major difference occurs just near the catalytic surface i.e. $\rho > 0.8$, since the catalytic (wall) reaction acts as a sink on the surface. The analysis shows that the effect of the reaction order on the concentration field is not important for the values of the parameters used.

Fig. 4(b) shows the concentration profiles for the case where there is a first order reaction on the catalytic surface and for different values of the D_{aw} number with $\alpha = 100$. This figure shows the effect of a variation in the Damkholer number, D_{aw} on the lateral concentration profiles at outlet of the reactor. It is observed that very little conversion occurs for the case of $D_{aw} = 0.1$ since the profiles for such a value of D_{aw} is almost the same as that for $D_{aw} = 0$. Also, as expected, the concentration of reactant decreases when increasing the value of D_{aw} number (see Eq. (61)). A value of $D_{aw} = 1$ yields a wall concentration of reactant at the outlet of the system of $C_w(1) = 0.88$ while when the D_{aw} is increase a hundred times, the concentration of reactant goes to a value of $C_w(1) = 0.06$. The effect of the increase of the conversion may be explained due to the effects of the reaction constant, $k_w W/D$. If one keeps W, D as constants, then an increase in the reaction constant, k_w implies that the power of the wall reaction increases. Hence, the concentration of reactant decreases in the system, or alternatively, the conversion in the reactor increases.

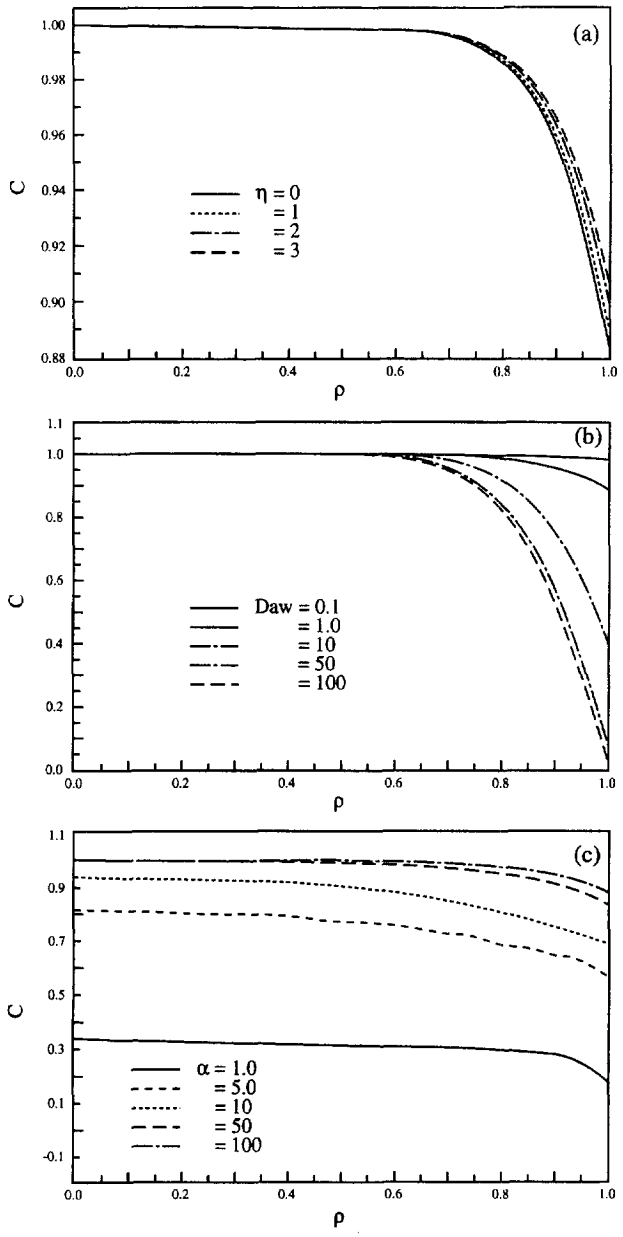

Fig. 4. Output radial concentration profiles for power-law kinetics for different values of the order (a), Da(b) and α(c).

Also, examination of Fig. 4(b) shows that the variation of concentration take place in the region near the catalytic surface of the system ($\rho > 0.55$), it implies that only a region of the system (close to the catalytic surface) is under the influence of the surface reaction for a given condition ($\alpha = 100$). As we increase the D_{aw} number, the effect of the reaction becomes larger.

Fig. 4(c) shows the effect of the residence time of the system on the concentration profiles through the parameter $\alpha(\alpha \equiv \text{PeGe})$ for a given D_{aw}. This parameter is varied between $\alpha = 1.0$ and $\alpha = 100$. The effect of the parameter can be interpreted in two different ways. For a given geometry and a value of the diffusion coefficient, when convection is stronger, the residence time is smaller and concentration of reactant in the system goes up. On the other hand, if the velocity of the fluid is constant, then a species with a small diffusion coefficients has less mass transported towards the catalytic wall, and the concentration of reactant increases. From Fig. 4(c) it can be seen that for the values of $\alpha < 50$ there are significant effects on the concentration profiles. Most of the profiles, for a given value of α, remains unchanged throughout the domain of the variable ρ and the most appreciable change occurs near the wall of the reactor, $\rho = 1$.

Fig. 5 shows the computational results for the case of a Langmuir–Hinshelwood reaction given by $D_{aw}C_w/(K + C_w)$ that occurs at the moving wall of the system. The calculations were performed using $\alpha = 100$ and $D_{aw} = 1$, and the value of K is varied within the range between $K = 0.01$ and $K = 100$. From Fig. 5(a), it can be seen that concentration profiles have the same qualitative shape as those computed using power-law kinetics. The lateral (Fig. 5(b)) concentration profiles show the most significant depletion in the reactant concentration near the wall ($\rho = 1$) in a region located in the range $0.7 < \rho < 1$. Fig. 2(b) shows the variation of lateral concentration with different values of K in the system ($\xi = 0.6$).

Presented in Fig. 5(a) are the axial concentration profiles at the wall positions ($\rho = 1$). As the value of K increases, the concentration profiles goes up. For example, the values of the concentration of reactant at the outlet ranges from 0.880 for ($K = 0.1$) to 0.330 (for $K = 100$). The result can be explained by analysing the expression for the reaction rate $D_{aw}C_w/(K + C_w)$, when K increases, the reaction rate becomes

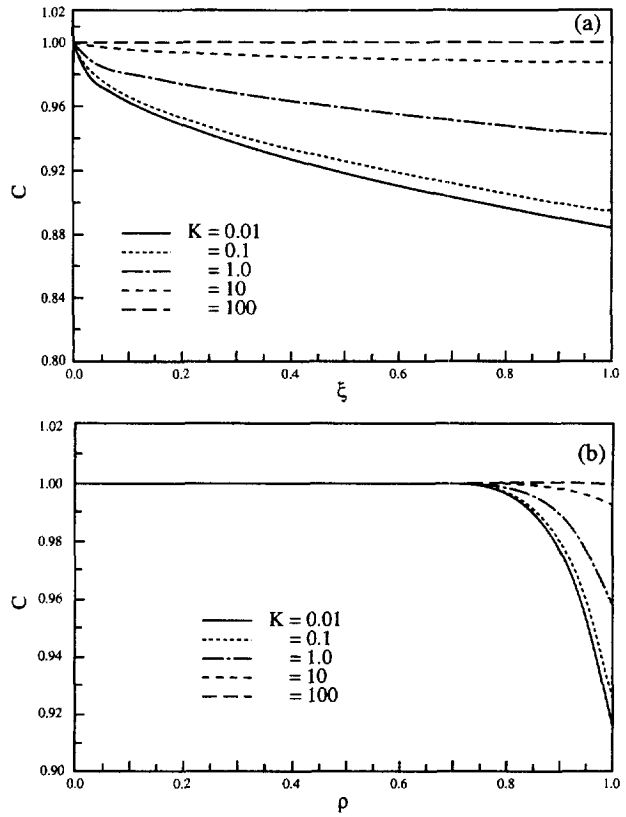

Fig. 5. (a) Axial (at $\rho = 1$) and (b) radial ($\xi = 0.6$) concentration profile for Langmuir–Hilshelwood kinetics for different values of k and for $\alpha = 100$ and $D_{aw} = 1$.

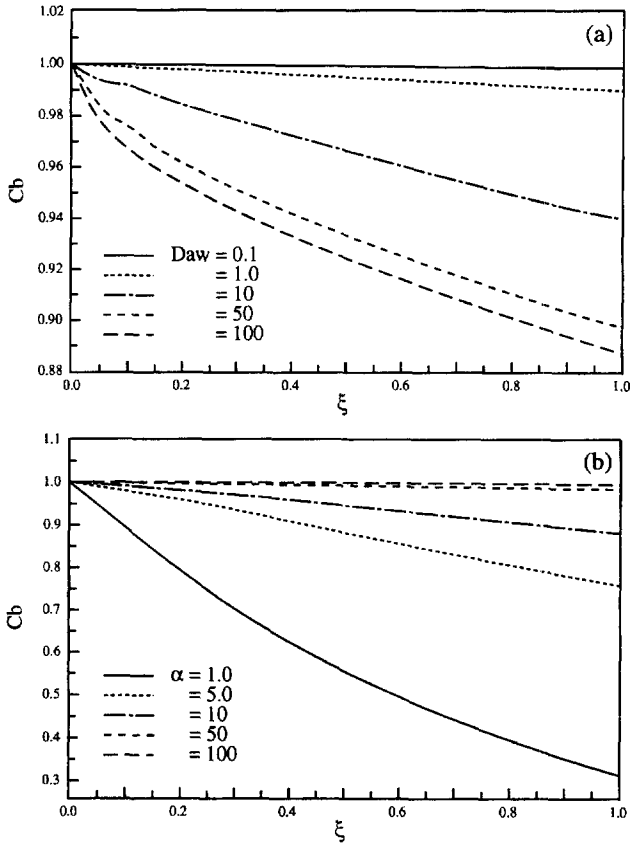

Fig. 6. Bulk concentration profiles for $\alpha = 100$ and different values of D_{aw} (a) and different values of α (b).

smaller indicating that the conversion of the reactant goes down. It is also noted from Fig. 5(a) and b, the concentration changes significantly when the value of K changes in $0.1 \leq K \leq 10$.

One important variable in the characterization of the system behaviour is the bulk concentration, $C_b(\xi)$. The definition of the bulk concentration is given [15]:

$$C_b(\xi) = \frac{\int_0^1 d\rho'\, \rho' C(\xi,\rho')}{\int_0^1 d\rho'\, \rho'} = 2\int_0^1 d\,\rho'\rho' C(\xi,\rho') \qquad (68)$$

For the case of first order reaction, the bulk concentration of reactant is given by

$$C_b(\xi) = 1 - \frac{D_{aw}}{2\alpha}\sum_{n=0}^{\infty}\frac{\phi_n^2(1)}{A_n^2}\int_0^{\xi}\exp[-\beta_n(\xi-\xi')]C_w(\xi') \qquad (69)$$

This equation is linear and, therefore, it could be solved analytically by using a series expansion procedure [27], however, it can also solve numerically using the approach previously described.

Fig. 6(a) and (b) shows a parametric analysis of the behaviour of the bulk concentration profile for different values for D_{aw} and different values of α. Computations for Fig. 6(a) are performed for $\alpha = 100$ while those in Fig. 6(b) for $D_{aw} = 1$. As the value of α is constant, the bulk concentration decreases with the value of D_{aw} increases. As shown in Fig. 6(b) when the value of α increases, the bulk concentration also increases.

5. Illustrations for the homogenous reaction case

The case of interest here is the system with homogeneous reaction that has a rate expression given by an arbitrary order n order for power-law kinetics. An analysis of some limiting situation, i.e. zero order reaction and first order reaction will also be performed. A numerical calculation of the concentration of reactant is also performed. For case of homogeneous reaction, the concentration field is affected by the parameters of the system (α, Da, n) and their influence will be discussed.

The general integral equation for the concentration is given by

$$C(\xi,\rho) = \int_0^1 \rho' G(x|0,\rho')\,d\rho' - \frac{1}{\alpha}\int_0^{\xi} d\xi' \int_0^1 d\rho'\, G(x|x')$$

$$\times \Omega[C(x')] - \frac{1}{\alpha}\int_0^{\xi} d\xi'\, G(x|\xi',1)\Omega_w[C(\xi',1)] \qquad (70)$$

For the analysis of the case under investigation, ξ is in the domain $0 \leq \xi \leq 1$.

The boundary condition at the fixed wall, $\rho = 0$ is $dC/d\rho = 0$ and at the moving wall, $\rho = 1$, the boundary condition is also given by $dC/d\rho = 0$ since that case considered here it is assumed that there is no reaction at the wall (i.e. $\Omega[C(\xi,1)] = 0$). Also, at the inlet of the system, a uniform distribution is assumed. Hence, the integral equation for the system described above reduces to

$$C(\xi,\rho) = 1 - \frac{1}{\alpha}\int_0^{\xi} d\xi' \int_0^1 d\rho'\, G(x|x')\Omega[C(x')] \qquad (71)$$

Homogeneous reaction of a generalized nth order has a kinetic equation of the following type

$$R[C'(x)] = kC'^n(x) \qquad (72)$$

where the integer $n (n \leq 0)$ may take the usual values 0, 1, 2, and 3. The non-dimensional form of Eq. (72) is

$$\Omega[C(x)] = \frac{W^2 k}{D} C^n(x) = \mathrm{Da}C^n(x) \qquad (73)$$

where $\mathrm{Da} \equiv W^2 k/D$ is the dimensionless group known as Damkholer number for the case of homogeneous reaction in the bulk. When the function $\Omega[C(x)]$ is replaced by the non-dimensional kinetic rate function given by Eq. (73), the concentration field $C(\xi,\rho)$ becomes

$$C(\xi,\rho) = 1 - \frac{\mathrm{Da}}{\alpha}\int_0^{\xi} \mathrm{d}\xi' \int_1^{1} \mathrm{d}\rho' G(\boldsymbol{x}|\boldsymbol{x}') C^n(\boldsymbol{x}')\, \mathrm{d}\rho' \tag{74}$$

where

$$G(\boldsymbol{x}|\xi') = \sum_{n=0}^{\infty}\left[\exp\left(\frac{\lambda_n^2}{\alpha}(\xi' - \xi)\right)\phi_n(e)\,\phi_n(\rho') \times A_n^{-2}\theta(\xi - \xi')\right] \tag{75}$$

In Eq. (74) the first term on the right hand side is the contribution by the inlet condition on the concentration profile (this is evaluated for the particular case of $C(0,\rho)) = 1$. The second term on the right hand side is the contribution from the homogeneous chemical reaction $\Omega[C(\boldsymbol{x})]$ to the system. Therefore, Eq. (74) is the formal solution for the homogeneous reaction case. For this equation some limiting cases can be identified. For example, for the particular situation of $n = 0$ Eq. (74) reduces to

$$C(\xi,\rho) = 1 - \left(\frac{\mathrm{Da}}{\alpha}\right)\xi - \mathrm{Da}\sum_{n=0}^{\infty}\frac{\phi_n(\rho)}{A_n^2\lambda_n^2} \times [1 - \exp(\beta_n\xi)]\int_0^{1} \mathrm{d}\rho'\, \phi_n(\rho') \tag{76}$$

The zero eigenvalue ($\lambda_0 = 0$) and the corresponding normalized zero eigenfunction ($\phi_0 = \sqrt{2}$) were used to give the second term on the right hand side of Eq. (76). These integrals can be calculated analytically by using the Airy functions $\phi_n(\rho)$) or, alternatively, computed numerically [28].

In order to characterize the concentration behaviour in the system, the bulk concentration, $C_b(\xi)$ need to be considered. The bulk concentration profile with respect to the axial coordinate of the system can be obtained by using the definition as follows

$$C_b(\xi) = \frac{\int_0^{1} \mathrm{d}\rho'\, \rho' C(\xi,\rho')}{\int_0^{1} \mathrm{d}\rho'\rho'} = 2\int_0^{1} \mathrm{d}\rho'\, \rho' C(\rho',\xi) \tag{77}$$

Substituting Eq. (76) into Eq. (77), the bulk concentration for homogeneous reaction with arbitrary order, n, is given by

$$C_b(\xi) = 1 - \left(\frac{2\mathrm{Da}}{\alpha}\right)\sum_{n=1}^{\infty}\frac{\gamma_n}{A_n^2}\int_0^{\xi} \mathrm{d}\xi' \times \exp[-\beta_n(\xi - \xi')]\int_0^{1} \mathrm{d}\rho'\, \phi_n(\rho') C^n(\xi'),\rho') \tag{78}$$

γ_n was defined previously in Eq. (54). By using the properties of the γ_n(see Eqs. (55) and (86)) where $n < 0$, $\gamma_n = 0$. Eq. (78) can be reduced to

$$C_b(\xi) = 1 - \left(\frac{2\mathrm{Da}}{\alpha}\right)\int_0^{\xi} \mathrm{d}\xi' \int_0^{1} \mathrm{d}\rho'\, \phi_n(\rho') C^n(\xi',\rho') \tag{79}$$

For the zero order limiting case, Eq. (79) becomes

$$C_b(\xi) = 1 - \left(\frac{2\mathrm{Da}}{\alpha}\right)\xi \tag{80}$$

From the definition of conversion of the system $\chi(\xi)$

$$\chi(\xi) = 1 - C_b(\xi) = \frac{2\mathrm{Da}}{\alpha}\xi \tag{81}$$

Eq. (81) suggests an interesting condition for the parameters of the system. Values of the parameters such that $2\mathrm{Da}/\alpha > 1$ will result in a total conversion (i.e. $\chi(\xi) = 1$) for the reactant before reaching the system outlet. On the contrary, the $2\mathrm{Da}/\alpha < 1$ will produce an output conversion level of the reactant less than 1. A value of $2\mathrm{Da}/\alpha = 1$ determines an optimal condition in the parameters that assures total conversion of the reactant at the outlet of the reactor.

Another limiting case is the first order homogeneous reactions (i.e. $n = 1$). In this situation, Eq. (78) is rewritten to become a linear integral equation given by

$$C(\xi,\rho) = 1 - \frac{\mathrm{Da}}{\alpha}\sum_{n=0}^{\infty}\frac{\phi_n(\rho)}{A_n^2}\int_0^{\xi} \mathrm{d}\xi' \exp[-\beta_n(\xi - \xi')] \times \int_0^{1} \mathrm{d}\rho'\, \phi_n(\rho)' C(\xi',\rho') \tag{82}$$

In order to illustrate the behaviour of the concentration profile of the reactant numerical computations have been performed on Eqs. (74) and (79) with different values of parameters of the system. Fig. 7 shows lateral concentration profiles for the first order reaction with α values in the range 1–100 and with Da changes from 0.1 to 100.

Fig. 7(a) shows the lateral concentration profiles for $\xi = 0.6$. The general trend of concentration profiles along the lateral coordinate is that all concentration profiles start from their lowest values at $\rho = 0$, and reach their highest value at $\rho = 1$. It is observed that the regions closer to $\rho = 0$ (i.e. the fixed wall) have a larger conversion than the ones near $\rho = 1$ (i.e. the upper wall system). The behaviour implies that the concentration distribution is strongly affected by the flow field as can be seen from the figures.

Fig. 7(b) shows the concentration distribution for a given $\mathrm{Da} = 1$, $n = 1$, with different values of α (from 1 to 100). The concentration of reactant decreases as the value of α decreases. When $\alpha > 50$, the variation of concentration of reactant is insignificant along the lateral coordinate ρ. Computed profiles show that the variation of values of α on the

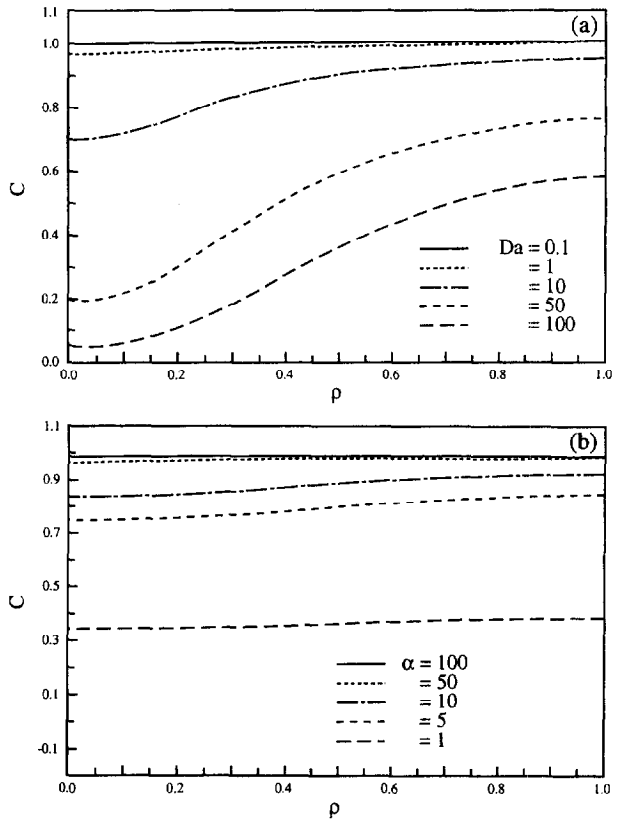

Fig. 7. Radial concentration profiles for the first order homogeneous reactions for a given volume of $\alpha = 100(a)$ and different values of Da(b): Idem (a) with different values of α and Da = 1.

concentration field is more significant for the axial concentration profile than the lateral concentration profile [13].

6. Illustrations for the case of simultaneous surface and homogeneous reaction

In this section, the solution for the case of simultaneous (bulk and wall) reactions with power law kinetics will be presented. Furthermore, analysis for the simple case of zero order will also be determined. Some numerical calculations regarding the illustration of the behaviour of concentration profiles will be included. The general integral solution for simultaneous reactions is given by Eq. (50) of Section 4.

From the mathematical point of view, Eq. (50) is more complicated than Eqs. (58) and (71) discussed in the previous sections since it requires the use of the three terms in the integral equation and, also requires an iteration procedure over both spatial variables (i.e. ρ and ξ) to obtain the solution. This equation can be reduced for the uniform inlet concentration i.e. $C(\xi=0)=1$, as shown in Sections 4 and 5. For this situation, the input terms reduce to unity. If an arbitrary order, n, for the power-law kinetics is used for the wall reaction (see Eq. (59)) as well as for the homogeneous reaction (see Eq. (74)), then Eq. (50) becomes

$$C(\xi,\rho) = 1 - \frac{D_{aw}}{\alpha}\int_0^{\xi} d\xi'\, G(x|1,\xi')C^n(1,\xi') - \frac{Da}{\alpha}\int_0^{\xi} d\xi' \int_0^{1} G(x|x')C^n(\xi',\rho')\, d\rho' \quad (83)$$

The first term on the right hand side of this equation is the effect of the inlet distribution, the second term is the contribution of the catalytic wall reaction, and the third term is the effect of the bulk reaction. This equation can also be solved by the methodology developed in Section 4 and applied previously in Sections 4 and 5 to the particular cases of catalytic wall reaction and homogeneous reaction, respectively.

By using the procedure previously outlined, the general solution for the zero order reaction for the case of simultaneous homogeneous and heterogeneous reactions is given by

$$C(\xi,\rho) = 1 - [2D_{aw} + Da]\left(\frac{\xi}{\alpha}\right) - \sum_{n=1}^{\infty}\frac{\phi_n(\rho)}{A_n^2\beta_n}\left[\frac{D_{aw}}{\alpha}\phi_n(1) + \frac{Da}{\alpha}\int_0^{1} d\rho'\, \phi_n(\rho') \times (1-\exp(-\beta_n\xi))\right] \quad (84)$$

Substituting Eq. (84) into the definition of the bulk concentration, Eq. (68) and using the properties of γ_n (see Eq. (55)), we obtain

$$C_b(\xi) = 1 - (2D_{aw} + Da)\frac{\xi}{\alpha} \quad (85)$$

Then, defining bulk conversion of the system, $\chi(\xi)$ leads to

$$\chi(\xi) = \frac{2D_{aw} + Da}{\alpha}\xi \quad (86)$$

As discussed in Section 5, the optimal point is obtained when

$$\frac{2D_{aw} + Da}{\alpha} = 1 \quad (87)$$

Eq. (83) is solved for the general kinetics (i.e. different from a zero order kinetics) by the methodology which is given in Section 2. Since Eq. (83) features wall reactions, the concentration profile, $C(\xi, \rho)$ will show the Gibbs phenomena in the region of $\rho = 1.0$. In order to smooth the effect of the Gibbs phenomena on the computation of the concentration profile, the procedure explained in Appendix A can be used to modify Eq. (83) and derive a new formula for an efficient computational approach similarly to what was obtained for catalytic (wall) reactions.

Fig. 8(a) and (b) shows the dimensionless lateral (Fig. 8(a)) and axial (Fig. 8(b)) concentration for $\alpha = 100$, $Da = D_{aw} = 1$ with $n = 0,1,2$ and 3 for both bulk and surface reactions. It can be seen from Fig. 8(a) that the lateral profiles

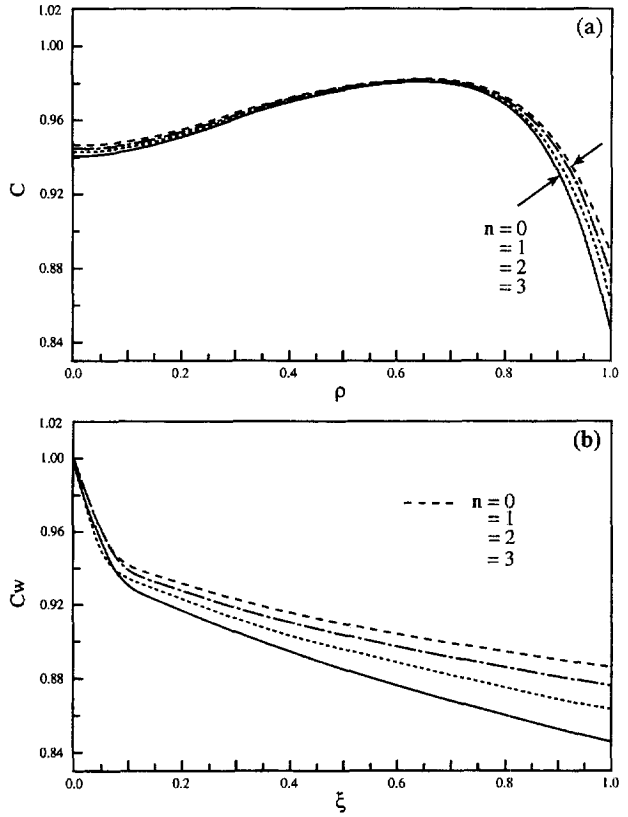

Fig. 8. (a) Radial and (b) axial concentration profiles for the case of simultaneous reactions for $\alpha = 100$, $D_{aw} = Da = 1$ and different order ($n = 1,2,3$).

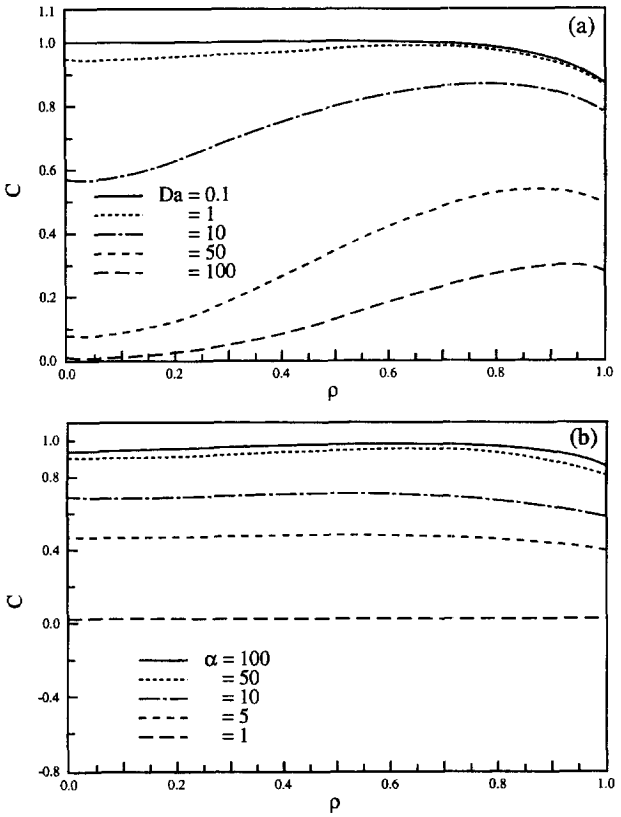

Fig. 9. Radial concentration for first order simultaneous reaction for $\alpha = 100$, $D_{aw} = 1$ with different Damkholer numbers, Da, (a) and (b) for $D_{aw} = Da = 1$ and with different values of α.

are very close to each other. And in this case, the biggest difference among the concentration profiles occurs near both ends, the moving wall and the fixed wall. This behaviour is caused by the *simultaneous reaction* situation that we consider here. Near the fixed wall, the concentration drop is mainly due to a longer residence time, however, close to moving wall, the concentration is affected by the catalytic surface reaction which occurs on the surface of the moving wall. The shape of concentration profile depend on parameters, Pe and Da. From Fig. 8(b), we can see that the concentration, for example, at the outlet of the system reaches a value of $C_w(1) = 0.874$ for the zero order reactions (i.e. for both of wall and bulk reactions), and a value of $C_w(1) = 0.885$ for simultaneously first order reactions.

Fig. 9(a) shows the lateral concentration distribution for the value of $D_{aw} = 1$, with different values of homogeneous reaction rate $Da = 0.1$, 1, 50, 100. It is shown in the figure, that as the value of Da increases the concentration of reactant decreases. The greater effect of in the drop in concentration values is seen near the fixed wall ($\rho = 0$) because of the distribution in the residence time values. Therefore, for the particular values of the parameters in this region, the homogeneous chemical reaction a dominant effect relative to the heterogeneous chemical reaction.

Fig. 9(b) shows the effect of the values of α on the concentration distribution for $D_{aw} = Da = 1$, and for the first order reactions. As we decrease the values of α, the concentration moves down. This is due to the residence time which is influenced by the velocity field. Also it is seen that the concentration profiles differ greatly for different values of the α when $\alpha < 50$. Fig. 9(b) shows the wall concentration along the lateral coordinate with different value of α. It is noted that for a small value of α, the wall concentration profile become less pronounced and it exhibits an almost linear trend of decay.

7. Summary and conclusions

The work of this paper is focused on the general mathematical formulation of the convective–diffusive mass transfer and reaction problem associated with Couette flow. An integral–spectral approach is developed in terms of integral equations by generating the approximate Green functions. The Green function is expanded in terms of the eigenvalues and eigenfunctions of the associated Stürm–Liouville problem that arise from the identification of the diffusion operator of the transport problem and is solved analytically by using Airy functions. The Green function has mathematical features common to all transport situations and, interestingly, it is independent of factors, such as the reaction sources, that are specific to each problem. These characteristics are very useful in avoiding repetitive computational effort when treating different cases and performing a parametric analysis as it is illustrated in this article. For example, the integral–spectral

methodology developed in this contribution is applied to cases with uniform inlet distributions and either catalytic wall reactions, homogeneous bulk reactions or simultaneous wall catalytic and bulk homogeneous reactions. The integral equation resulting from inverting the differential problem is the formal solution to the differential reactor system and it requires a computational (i.e. iterative) procedure to obtain the concentration profiles except in the case of zero order reactions. For this particular case, analytical solutions are derived from the general integral solution and various a priori conditions for the parameter space (α, Da, D_{aw}) can be written for such a solution. Also, the integral equation features the contribution of the three main physical factors of the reactor problem, i.e. the inlet distribution of reactants, the catalytic reaction at the wall, and the homogeneous chemical reaction in the bulk. These three different conditions can be clearly identified in the final equation from which particular cases can be derived as well.

Concentration profiles have been obtained numerically in the system. The results indicate the significant effect of heterogeneous chemical reactions only near the wall of the reactor, for a wide range of parameters; i.e. Peclet number Pe, homogeneous reaction parameter Da and wall reaction parameter D_{aw}.

For the case of catalytic reaction at the wall, concentration profiles have been computed for a variety of situations and for two different types of kinetics, i.e. power-law and Langmuir–Hinshelwood. The calculations show that for the power-law kinetics, the effect of reaction order, n on the concentration field is insignificant.

Due to the non-homogeneous boundary conditions for the case of wall catalytic reactions, the Gibbs phenomenon results from the Fourier expansions associated with the Green function. This phenomenon must be significantly reduced in order to obtain the concentration profiles. The technique which is applied here for such a purpose is based on closed sums of Fourier problems featuring zero-order kinetics. The proposed technique is an alternative to the classical Lanczos methodology to smooth the impact of the Gibbs phenomenon in Fourier expansions. The computational technique used in this case is well suited for reaction occurring at the wall. For example, the usual two dimensional problem is solved (iteratively) by using a one dimensional problem, i.e. the unknown is only the concentration at the wall. This aspect reduces considerably the computer requirements and it leads to an efficient way of solving the differential model.

Computations with illustrations for a variety of situations were also performed for the simultaneous bulk reaction and catalytic wall reaction case. The computations show that, for the values of the parameters used in the analysis, the homogeneous reaction has an important effect on the shape of the concentration profile. The wall reaction only affects the shape of the concentration profile near the wall channel. This can also be seen as the effect of the distribution of the residence time in the reactor. Due to the linear nature of the convective velocity, such a residence time is larger near the steady wall and smaller near the moving wall. The computations performed in this paper show that the integral–spectral method works for a number of cases in convective diffusive transport in Couette flows. The method can also be extended to even more complex situation such as multicomponent and non-uniform inlet distributions or non-uniform catalytic activity at the wall. Some of these cases will be the subject matter of future communications.

8. Nomenclature

A_n	normalization coefficient for Stürm–Liouville Problem
C	concentration, non-dimensional
c'	molar concentration, dimensional
c	non-dimensional concentration
D	diffusivity of reactant species
Da	Damkholer number, bulk reaction
D_{aw}	Damkholer number, wall reaction
Ge	geometrical parameter
H	width of the channel, dimensional
H	parabolic operator defined in Eq. (14)
I_n	integral function of eigenfunctions
k	absorption constant
L	length of the channel, dimensional
Pe	Peclet number, mass transfer UH/d
$V(y)$	hydrodynamic velocity profile, dimensional

Greek letters

α	parameter (PeGe), non-dimensional
β_n	λ_n^2/α, constant related to the eigenvalue λ_n
λ_n	nth eigenvalue of the Stürm–Liouville problem
$\phi_m(\rho)$	eigenfunction of the Stürm–Liouville system
Ω	reaction rate, non-dimensional
Ω_w	reaction rate (wall reaction), non-dimensional
ρ	lateral coordinate, non-dimensional
ξ	axial coordinate, non-dimensional

Subscripts

w	wall
ρ	derivative with respect to radial coordinates

Acknowledgements

One of us (ZC) received partial financial support from the office of Graduate Studies of Florida A&M University during the period of this research project. Such support is gratefully acknowledged

Appendix A

The term associated with the reaction at the wall in the formal integral solution can be re-written as follows

$$\hat{O}_w=\frac{1}{\alpha}\sum_{n=0}^{\infty}\frac{\phi_n(1)\phi_n(\rho)}{A_n^2}\int_0^{\xi}\exp(-\beta_n\xi')\Omega_w(\xi',1)\,d\xi'$$

$$=\frac{1}{\alpha}\sum_{n=0}^{N}\frac{\phi_n(1)\phi_n(\rho)}{A_n^2}\exp(-\beta_n\xi')\int_0^{\xi}\exp(\beta_n\xi')\times\Omega_w(\xi',1)\,d\xi'+\frac{1}{\alpha}\sum_{n=N+1}^{\infty}\frac{\phi_n(1)\phi_n(\rho)}{A_n^2}\times\exp(-\beta_n\xi')\int_0^{\xi}\exp(\beta_n\xi')\Omega_w(\xi',1)\,d\xi' \quad (A1)$$

Now, an asymptotic expression for the second term on the right hand side of Eq. (A1) will be derived. By performing an integration by parts, this term can be rewritten as

$$\hat{R}=\frac{1}{\alpha}\sum_{n=N+1}^{\infty}\frac{\phi_n(1)\phi_n(\rho)}{A_n^2}\exp(-\beta_n\xi)\int_0^{\xi}\exp(-\beta_n\xi')\times\Omega_w(\xi',1)\,d\xi'$$

$$=\sum_{n=N+1}^{\infty}\frac{\phi_n(1)\phi_n(\rho)}{A_n^2\lambda_n^2}[\Omega_w(\epsilon,1)-\Omega_w(0,1)\times\exp(-\beta_n\xi)]-\sum_{n=N+1}^{\infty}\frac{\phi(\rho)\phi_n(1)}{A_n^2\lambda_n^2}\int_0^{\xi}\times\exp(\beta_n(\xi'-\xi))\Omega'_{w\xi'}(\xi',1)\,d\xi' \quad (A2)$$

If the number, N, is chosen such that $\beta_N\Delta\xi\gg 1$, where $\Delta\xi$ is the step length for ξ, them we have

$$\exp(-\beta_n\xi)\approx\theta(\xi) \quad (A3)$$

$$\exp(-\beta_n(\xi-\xi'))\approx\theta(\xi'-\xi) \quad (A4)$$

where, $\theta(\xi)$ is a special function which is defined in a real space as

$$\theta(\xi)=\begin{cases}1 & \text{if } \xi=0\\ 0 & \text{otherwise}\end{cases}$$

Then, Eq. (A1) can be further simplified as

$$\hat{R}\approx\sum_{n=N+1}^{\infty}\frac{\phi_n(1)\phi_n(\rho)}{A_n^2\lambda_n^2}[\Omega_w(\xi,1)-\Omega_w(0,1)\theta(\xi)]-\sum_{n=N+1}^{\infty}\frac{\phi_n(1)\phi_n(\rho)}{A_n^2\lambda_n^2}\Omega_{w\xi'}(\xi,1)\int_0^{\xi}\times\exp(\beta_n(\xi'-\xi))\,d\xi'$$

$$=\sum_{n=N+1}^{\infty}\frac{\phi_n(\rho)\phi_n(1)}{A_n^2\lambda_n^2}[\Omega_w(\xi,1)-\Omega_w(0,1)\theta(\xi)]-\sum_{n+N+1}^{\infty}\frac{\phi_n(\rho)\phi_n(1)}{A_n^2\lambda_n^2}[\alpha\Omega_{w\xi}(\xi,1)(1-\theta(\xi))] \quad (A5)$$

Now, both terms in the equation have been expressed as the products of a ρ-related function and a ξ-related function. The ρ-related parts are the series expansions of eigenfunctions which are independent of the parameters chosen in the calculation. It is convenient to define the following functions

$$\psi_c^{(1)}(\rho)=\sum_{n=1}^{\infty}\frac{\phi_n(\rho)\phi_n(1)}{A_n^2\lambda_n^2} \quad (A6)$$

$$\psi_c^{(2)}(\rho)=\sum_{n=1}^{\infty}\frac{\phi_n(\rho)\phi_n(1)}{A_n^2\lambda_n^4} \quad (A7)$$

$$\psi_b^{(1)}(\rho,N)=\sum_{n=1}^{\infty}\frac{\phi_n(\rho)\phi_n(1)}{A_n^2\lambda_n^2} \quad (A8)$$

$$\psi_b^{(2)}(\rho,N)=\sum_{n=1}^{\infty}\frac{\phi_n(\rho)\phi_n(1)}{A_n^2\lambda_n^4} \quad (A9)$$

Substituting Eqs. (A6)–(A9) into Eq. (A5) yields the following relationship

$$\hat{R}=[\psi_c^{(1)}(\rho)-\psi_b^{(1)}(\rho,N)][\Omega_w(\xi,1)-\Omega_w(0,1)\theta(\xi)]-\alpha[\psi_c^{(2)}(\rho)-\psi_b^{(2)}(\rho,N)]\Omega'_{w\xi}(\xi,1)[1-\theta(\xi)] \quad (A10)$$

A close form expression $\psi_c^{(1)}(\rho)$ was derived by Mills [24] and it can be written as

$$\psi_c(\rho)=A_0[V_0(\rho^4/12-\rho^3/6]+A_2 \quad (A11)$$

where for the case of interest

$V_0=0$
$A_0=6.0/(V_0-3.0)$
$A_2=36(V_02/280-V_0/40+1/3)/V_0-3)^2$

In Eq. (A10), the value of the second term can be shown to be much smaller than the first term, if adequate number of terms are taken. Therefore, for example, if $|1/\beta_n|=|\alpha/\lambda_n^2<1$, then the following relationship can be written

$$|\alpha[\psi_c^{(2)}(\rho)-\psi_b^{(2)}(\rho,N)|=\left|\alpha\sum_{n=N+1}^{\infty}\frac{\phi_n(1)\phi_n(\rho)}{A_n^2\lambda_n^4}\right|<\left|\frac{\alpha}{\lambda_{N+1}^2}\right|\left|\sum_{n=N+1}^{\infty}\frac{\phi_n(0)\phi(\rho)}{A_n^2\lambda_n^2}\right|=\left|\frac{\alpha}{\lambda_{N+1}^2}\right||[\psi_c^{(1)}(\rho)-\psi_b^{(1)}(\rho,N)]| \quad (A12)$$

In consequence, the second term is smaller than the first term by a factor of β_{N+1}. The computation of the correction part is then further reduce to the calculation of

$$\tilde{R}\approx[\psi_c^{(1)}(\rho)-\psi_b^{(1)}(\rho,N)][\Omega_w(1,\xi)-\Omega(0,\xi)\theta(\xi)] \quad (A13)$$

Thus, for the case of only heterogeneous reaction, at the wall the integral Eq.(26) becomes

$$C(\xi,\rho) = 1 - (\psi_c^{(1)}(\rho) - \psi_b^{(1)}(\rho,N))(\Omega_w(1,\xi) - \Omega_w(0,\xi)\theta(\xi)) - \frac{1}{\alpha}\sum_{n=0}^{N}\frac{\phi_n(1)\phi_n(\rho)}{A_n^2}e^{-\beta_n\xi}\int_0^{\xi} \times \exp(\beta_n\xi')\Omega_w(\xi',1)\,d\xi' \quad (A14)$$

This nonlinear integral equation was solved by the iterative scheme proposed in previous Section 2 with $N = 10$–20. After this correction, the fluctuations in the concentration profile were drastically reduced for a wide range of parameters values of the system and for the same number of eigenvalues.

References

[1] F.A. Cleland, R.H. Wilhelm, Diffusion and reaction in viscous-flow tubular reactor, AIChE J. 2 (1956) 489.

[2] H.A. Lauwerier, A diffusion problem with chemical reaction, Appl. Sci. Res. A8 (1959) 366.

[3] J.S. Dranoff, An eigenvalue problem arising in mass and heat transfer studies, Math. Comput. 15 (1962) 406.

[4] R.V. Poirier, R.W. Carr, J. Phys. Chem. 75 (1971) 1953.

[5] P.J. Ogren, Analytical results for first-order kinetics in flow tubes reactors with wall reactions, J. Phys. Chem. 79 (1975) 1749.

[6] W.S. Solbrig, D. Gidaspow, Convective diffusion in a parallel plate duct with one catalytic wall, laminar flow, first order reaction, Can. J. Chem. Eng. 45 (1967) 35.

[7] B. Levich, Physicochemical Hydrodynamics, Prentice-Hall, Englewood Cliffs, NJ, 1967.

[8] M.M. Denn, Process Fluid Mechanics, Prentice Hall, Englewood Cliffs, NJ, 1980.

[9] T. Papanastaciou, Applied Fluid Mechanics, Prentice Hall, Englewood Cliffs, NJ, 1993.

[10] E.N. Lightfoot, Transport phenomena in living systems, J. Wiley & Son, New York, 1974.

[11] P. Arce, A.E. Cassano, H.A. Irazoqui, The tubular reactor with laminar flow regime: An integral equation approach, Comput. Chem. Eng. 2 (11) (1988) 1103.

[12] P. Arce, B.R. Locke, Transport and reaction: An integral equation approach. Mathematical formulation and computational approaches, in: J. Menon (ed.), Research Trends in Chemical Engineering, vol. 2, Council of Scientific Information, Vilayil Gardens, Trivandrum, India, 1994, pp. 89–158.

[13] P. Arce, B.R. Locke, I.M.B. Trigatti, An integral–spectral approach for reacting Poiseuille flows, AIChE J. 42 (1) (1996) 23.

[14] P. Arce, An integral–spectral formulation for convective-diffusive transport in a packed-bed with adsorption at the wall and bulk reaction, Chem. Engr. Comm. 138 (1995) 113.

[15] R.B. Bird, W.E. Stewart, E.N. Lightfoot, Transport Phenomena, Wiley, New York, 1960.

[16] R. Haberman, Elementary Partial Differential Equations, Prentice-Hall, Englewood Cliffs, NJ, 1987.

[17] H.F. Weinberger, Introduction to Partial Differential Equations, Wiley, New York, 1966.

[18] Z. Chen, P. Arce, B.R. Locke, Convective–diffusive transport with a wall reaction in Couette flows, Chem. Eng. J. 61 (1996) 63.

[19] Abramowitz Stegun, Mathematical Handbook, Dover Publications, New York, 1970.

[20] R. Courant, D. Hilbert, Methods of Mathematical Physics, Wiley–Interscience, New York, 1953.

[21] M. Golberg, Solution Methods for Integral Equations, 2nd Edition, Plenum Press, New York, 1990.

[22] P. Linz, Numerical Methods for Volterra Integral Equations with Singular Kernels, SIAM Jr. of Numerical Analysis 6(3) (1969) 365.

[23] M.E.A. El-Tom, Efficient algorithms for volterra integral equations of second kind, Computing 14 (1969) 153.

[24] M. Mills, Asymptotic solutions for convective–diffusive heat transfer problems in Couette flows, Honors Thesis, Florida State University, 1993.

[25] J.J. Carberry, Catalytic Reaction Engineering, McGraw-Hill, New York, 1977.

[26] V.D. Dang, M. Steinberg, Convective–diffusion with homogeneous and heterogeneous reactions, J. Phys. Chem. 84 (1980) 214.

[27] V. Volterra, Theory of Functional and of Integral and Integro-Differential Equations, Dover Publications, New York, 1959.

[28] Z. Chen, Convective–diffusive mass transfer with chemical reaction in couette flow, Ms.Sc. Thesis, Florida A&M University, 1994.

[29] W.S. Charles, D. Gidaspow, Convective diffusion in a parallel plate reactor with one catalytic wall-laminar flow—arbitrary reaction order, Presented at the XXXVI Congress Internationale de Chemie Industrialle, Bruxelles, September 10–21, 1966 (Paper 702).

[30] B. Lebedev, Special Functions and Their Applications, Dover Publications, New York, 1972.